



Available online at www.sciencedirect.com

ScienceDirect

Advances in Space Research 63 (2019) 417–431

**ADVANCES IN
SPACE
RESEARCH**
(a COSPAR publication)
www.elsevier.com/locate/asr

Characteristics of GOCE orbits based on Satellite Laser Ranging

Dariusz Strugarek ^{a,*}, Krzysztof Sośnica ^a, Adrian Jäggi ^b

^a Institute of Geodesy and Geoinformatics, Wrocław University of Environmental and Life Sciences, Grunwaldzka 53, 50-357 Wrocław, Poland

^b Astronomical Institute, University of Bern, Sidlerstrasse 5, 3012 Bern, Switzerland

Received 12 May 2018; received in revised form 21 August 2018; accepted 21 August 2018

Available online 30 August 2018

Abstract

The Gravity field and steady-state Ocean Circulation Explorer (GOCE) was the first European Space Agency's (ESA) Earth Explorer core mission. Through its extremely low, about 260 km above the Earth, circular, sun-synchronous orbit, the satellite gained high spatial resolution and accuracy gravity gradient, and ocean circulation data. Global Positioning System (GPS) receivers, mounted on the spacecraft, allowed the determination of reduced-dynamic and kinematic GOCE orbits, whereas Laser Retroreflector Array (LRA) dedicated to Satellite Laser Ranging (SLR) allowed an independent validation of GPS-derived orbits. In this paper, residuals between different GPS-based orbit types and SLR observations are used to investigate the sensitivity and the influence of solar, geomagnetic, and ionospheric activities on the quality of kinematic and reduced-dynamic GOCE orbits. We also analyze the quality of data provided by individual SLR sites, by detecting time biases using ascending and descending sun-synchronous GOCE orbit passes, and the residual analysis of the measurement characteristics, i.e., the dependency of SLR residuals as a function of nadir and horizontal angles. Results show a substantial vulnerability of kinematic orbit solutions to the solar F10.7 index and the ionospheric activity measured by the variations of the Total Electron Content (TEC) values. The sensitivity of kinematic orbits to the three-hour-range KP index is rather minor. The reduced-dynamic orbits are almost insensitive to indices describing ionospheric, solar, and geomagnetic activities. The investigation of individual SLR sites shows that some of them are affected by time bias errors, whereas other demonstrate systematics, such as a dependency between observation residuals and the satellite nadir angle or the horizontal azimuth angle from the SLR station to the direction of the satellite.

© 2018 COSPAR. Published by Elsevier Ltd. All rights reserved.

Keywords: GOCE; SLR; Ionosphere; Solar activity; Orbit determination

1. Introduction

The Gravity Field and Steady-State Ocean Circulation Explorer (GOCE) was the first European Space Agency's (ESA) Earth Explorer core mission (Drinkwater et al., 2006), as an effect of the "Living Planet Programme" strategy and plans for the Earth Observation in the 21st century which considered atmosphere, Earth surface and interior,

physical climate, geosphere/biosphere, and anthropogenic impact (ESA, 1998). The mission's main objective was to obtain gravity gradient and ocean circulation data with high spatial resolution and accuracy. GOCE was equipped with a three-axis gradiometer for determining the Earth's gravity field with an unprecedented accuracy of 1 mGal, and the geoid with an accuracy of 1 cm, both at a spatial resolution of 100 km (Rummel et al., 2002; Floberghagen et al., 2011). During almost the entire GOCE mission, the Low Earth Orbit (LEO) determination and gradiometer measurements supplementation was performed by one dual-frequency Lagrange GPS receiver, which allowed for satellite-to-satellite tracking in the high-low (SST-hl) mode

* Corresponding author.

E-mail addresses: dariusz.strugarek@igig.up.wroc.pl (D. Strugarek), krzysztof.sosnica@igig.up.wroc.pl (K. Sośnica), adrian.jaggi@aiub.unibe.ch (A. Jäggi).

(Drinkwater et al., 2006; Zin et al., 2006). Moreover, a Satellite Laser Ranging (SLR) Retroreflector Array (LRA) was mounted on the spacecraft that consisted of seven corner cubes (Bock et al., 2014). Observations to retroreflectors were improved with several models of azimuth-nadir dependent range corrections provided by Montenbruck and Neubert (2011), which allowed correcting SLR data and further verifying the orbit validation (Bock et al., 2014).

SLR is an optical-based technique typically used for determining geocenter motion, station coordinates, scale and origin of the International Terrestrial Reference Frame, Earth rotation parameters, performing precise orbit determination, and orbit validation (e.g., Pearlman et al., 2002; Altamimi et al., 2011). The main measurement principle of SLR is based on registration of time-of-flight of laser signal, from station telescopes to the retroreflector mounted on a satellite, where a laser pulse is reflected back to the detector at the station. Multiplying this “two-way” time interval by the speed of light, the half of the resulting value gives an approximated range. The obtained range has to be corrected taking into account various effects, such as atmospheric refraction, relativistic effects, LRA offset biases at the station (for details related to corrections applied on SLR observations to LEO see, e.g., Arnold et al., 2018). SLR residuals may be considered as differences between ranges obtained from SLR-based station-satellite range measurements and ranges computed from models or derived from orbit solutions.

GPS-based GOCE orbital parameters are predominantly affected by GPS signal errors, which are mostly caused by ionospheric variations. The signal propagation effect is due to the large sensitivity of GPS signals to ionosphere activities in different ionospheric layers of the signal path between the GPS and GOCE satellites. The largest error is caused by the signal delay (GPS code) and advance (GPS phase) and by fast changes in the ionosphere itself (scintillations). The signal delay and advance are taken into account by using the ionosphere-free linear combination of GPS observations collected on two frequencies (Bock et al., 2014) and accounting for the higher order effects using additional models (e.g., Hadas et al., 2017). SLR measurements are fully insensitive to the ionospheric delay. Therefore, large errors of SLR observations can be assigned to affected GOCE orbits because the optical SLR signal is not subject to any temporal variations or scintillations inside the ionosphere. SLR observations can thus be used as an independent way to assess the quality of GOCE orbits and the sensitivity of GPS signal data used for determination of GOCE orbits to the ionospheric activity.

In Section 3, we analyze residuals between SLR and two types of GPS-based orbit solutions: reduced-dynamic (Wu et al., 1991; Jäggi et al., 2006) and kinematic (Švehla and Rothacher, 2005). In Section 4, we compare the mean SLR residuals to the solar field activity index: F10.7 Solar Radio Flux, the Total Electron Content (TEC) related to the ionospheric activity, and the magnetic field activity

index KP. We also show the analysis of annual SLR residual statistics for each station and the analysis of station residuals w.r.t. the nadir angle and the horizontal azimuth angle of the observations. At the end of this section, we show a method for the detection of SLR biases using differences of SLR residuals from ascending and descending passes of satellites in sun-synchronous orbits. Results from this study may constitute a basis for future modeling and determination of systematic errors which affect both the GNSS and SLR observations to LEO.

2. GOCE mission overview

GOCE was launched on March 17, 2009. The mission may be divided into several mission phases: short-time launch and early orbit phase, commissioning (began in March 2009, ended in September 2009), routine phase (ended in July 2012), low orbit operations campaign (ended in September 2013), and de-orbiting and re-entry (last 2 months of the mission) which lasted until 11 November 2013 (GOCE Flight Control Team, 2014). Most of the SLR observations for this study were taken during the routine phase of the GOCE mission, where the mean altitude (mean distance from the geocenter minus the Earth radius at the equator) was at the level of about 260 km (Jäggi et al., 2011).

2.1. GOCE orbit characteristics

GOCE had an extremely low, about 260 km above Earth, circular, sun-synchronous orbit with an inclination of 96.6° which implies two, high-velocity daily passes above the same area: one pass during the dawn at about 6 am, and the second during the dusk at around 6 pm local time. During the dawn pass, GOCE was orbiting southward, along with the descending pass, whereas during the dusk passes the satellite moved northward with respect to the observer on the ground. The direct visibility of the GOCE satellite was possible for up to 3 ascending and descending passes for SLR stations which have very few obstacles, such as trees and buildings, at low elevation angles. A full Earth coverage required 979 satellite revolutions, which took approximately 61 days (Jäggi et al., 2011). Orbit altitude through the entire GOCE mission was lowered from 280 km to 230 km and for the final re-entry to about 170 km (GOCE Flight Control Team, 2014).

2.2. GPS-based orbits for GOCE

The precise orbit products for GOCE were operationally provided by the Astronomical Institute of the University of Bern (AIUB; Bock et al., 2014) and the Delft University of Technology (TU Delft; Visser et al., 2009) during the mission. In this research, we use SLR residuals to two kinds of GPS-based precise science orbits (PSO): reduced-dynamic (RD) and kinematic (KIN) orbits generated by AIUB (Bock et al., 2014). The GOCE PSO orbit determination

process uses the Precise Point Positioning (PPP) method with undifferenced ionosphere-free phase processing of the GPS observations. For both orbit types the same GPS measurement models (excluding sampling interval), reference frame and estimation methods were used: GOCE Phase Center Offsets and Variations (PCO, PCV; [Bock et al., 2011](#)), Center for Orbit Determination in Europe (CODE) Earth rotation parameters, final GPS ephemerides and 5 s clocks ([Dach et al., 2009](#); [Bock et al., 2009](#)) with the GOCE star tracker quaternions for a proper altitude determination. For the RD solutions, additional gravitational and empirical accelerations were applied. Detail information about employed dynamical and measurement model can be found in [Bock et al. \(2014\)](#).

In general, the KIN solution is represented as a discrete satellite position which disobeys the equation of motion and is determined epoch-wise. Each position is estimated for each measurement epoch considering the transformation matrix from the Earth-fixed to the inertial frame, a known antenna phase center offset, and a satellite center of mass position ([Jäggi, 2007](#)). It is a purely geometrical approach without using any information about the LEO satellite dynamics so that positions are fully independent of the force models used for LEO orbit determination ([Švehla and Rothacher, 2005](#)). The RD orbit is based on a solution that makes use of both the geometric strength of the GPS observations (kinematic) and the fact that satellite trajectories are particular solutions of a deterministic equation of motion (dynamic). This technique introduces additional pseudo-stochastic orbit parameters to the deterministic equation of motion ([Jäggi, 2007](#)) to absorb the not explicitly modeled, non-conservative forces, such as atmospheric drag, solar radiation pressure, Earth albedo and infrared radiation pressure. In total, the RD orbits heavily depend on the force models such as gravitational or non-gravitational models, whereas pseudo-stochastic orbit parameters absorb also some gravitational orbit perturbations, which is why they cannot be used, e.g., for an independent gravity field recovery ([Jäggi et al., 2008](#)).

3. Using the SLR technique for the orbit examination

Nominally, the SLR technique is used for determining time-varying geocenter coordinates, Earth orientation parameters (polar motion and length of day), coordinates and velocities of the SLR tracking stations, static and time-varying coefficients of the very long wavelength part of the Earth's gravity field, fundamental physical constants, and the global scale of the global reference frame ([Pearlman et al., 2002](#)). However, SLR can also be used for the estimation of the satellite microwave antenna offsets, independent orbit validation of all satellites equipped with laser retroreflector arrays ([Arnold et al., 2018](#)) or improvement analysis. Moreover, SLR can be used to assess the GPS-derived orbit quality during severe geomagnetic conditions or other orbit perturbing effects ([Willis et al., 2005, 2016](#)).

3.1. SLR validation of GPS-derived GOCE orbits

The SLR orbit validation is typically based on the residual analysis with the computation of statistic indices. Laser observations to GOCE GPS-based orbits were used by [Bock et al. \(2014\)](#), who obtained for the earlier mission period, mean and root-mean-square error (RMSE) values at the level of 0.18 ± 1.84 cm and 0.10 ± 2.42 cm for RD and KIN orbits, respectively. In a further analysis, the authors also compared RD with KIN orbits for 3D, radial, along-track and out-of-plane directions. The obtained results were compared against TEC and the corresponding percentage of missing L2 and KIN positions values, which showed a large correlation above 0.7. Moreover, [Bock et al. \(2014\)](#) showed large differences (at 5-cm level) between GPS-based orbit types at polar regions for descending and ascending GOCE passes. [Bruinsma et al. \(2017\)](#) used 49 observations collected by three SLR stations to validate GOCE orbits in the last three weeks of the mission, i.e., in the re-entry phase. The mean values and the RMSE of residuals for KIN orbits were at the level of -5.77 and 5.83 cm for Zimmerwald (7810), 3.87 and 3.94 cm for Monument Peak (7110), and -2.00 and 2.05 cm for Yarragadee (7090), respectively.

3.2. GOCE GPS-SLR residual characteristics

SLR measurements to high-orbiting satellites are sensitive mostly to the radial direction. However, extremely low GOCE orbits result in SLR tracking mostly for high nadir angles (at $60\text{--}70^\circ$), thus show sensitivity in the along-track when taking the north-south station direction to the satellite, and cross-track when taking the east-west station direction to the satellite ([Jäggi et al., 2011](#), [Arnold et al., 2018](#)). This may allow detecting potential systematic errors in all directions, when analyzing long time series of SLR data.

GPS-SLR residuals were calculated for this analysis using the Bernese GNSS Software ([Dach et al., 2015](#)). Residuals are calculated as a difference between SLR-based ranges and the range calculated in SLRF2005 ([Luceri and Bianco, 2008](#)) and SLRF2008 ([ILRS, 2016](#)), as station-satellite vectors derived from RD and KIN orbits. Ranges were transformed to the corresponding reference frames of the GPS and GOCE orbits IGS05/IGS08 ([Rebischung et al., 2012](#)) as a tie reference between SLR and GNSS products. For SLR ranges several delay corrections need to be taken into account: troposphere delay, described by [Mendes and Pavlis \(2004\)](#), site displacement loading and relativistic effects, modelled in the International Earth Rotation and Reference Systems Service (IERS) Conventions, and LRA offsets and their variability ([Montenbruck and Neubert, 2011](#)) and additional corrections recommended by the International Laser Ranging Service (ILRS) Analysis Standing Committee. [Arnold et al. \(2018\)](#) provide an overview of all corrections that have to be taken into account when using SLR to validate

LEO orbits. Moreover, there may occur some unmodeled effects, such as station and satellite systematic errors: range biases and time biases which affect single station-satellite laser measurements.

At the beginning of the mission, only a few SLR sites performed observations to GOCE, which was caused by the insufficient quality of orbit predictions. The situation changed when AIUB launched the GOCE orbit prediction service in October 2009 (Jäggi et al., 2011). The GOCE normal points were generated on the basis of SLR full rate observations contained in bins of 5 s. Such a short period was dictated by the very high relative speed of the satellite with respect to the SLR ground stations.

3.3. Time bias issue in laser ranging observations

A time bias is an error in consequence of a wrong synchronization of time or frequency technologies used at SLR sites that causes a difference between the observed and real position of the satellite at measurement time (Otsubo et al., 2018). Inhomogeneous equipment mounted at stations such as clocks, event timers, detectors, electronic devices, distribution cable lengths, may cause accuracy issues. Typical requirements for laser ranging station demand few to dozen picosecond level accuracy for the time interval of the detector work, one pulse per second (1-pps) generator parameters and nanosecond-level accuracy for long-term parameters like offset between 1-pps and National realization of Universal Time Coordinated (UTC), (Samain et al., 2015). The ILRS requires that the time synchronization limit is 100 ns for SLR sites (Pearlman et al., 2002). Time biases at the SLR stations may be erroneously assigned to systematic orbit errors in the along-track component when using SLR observations for LEO orbit validation (Otsubo et al., 2018).

In recent studies, Exertier et al. (2017, 2018) used the non-common-view method in time transfer technique for time scale comparison to detect time biases at SLR stations. They used the Time Transfer by Laser Link (T2L2) space experiment on-board the Jason-2 satellite for the years 2013 until 2016. The Grasse (7845) site was chosen as master reference station to synchronize other station clocks, due to a 5 ns tie to UTC. Some sites exhibited long-term stability at the level of less than 100 ns (Herstmonceux, Greenbelt), for other sites, 100–200 ns phase jumps occurred (e.g. in Grasse) or a typical time bias behavior occurred, even at few μ s-level (e.g., in Hartebeesthoek).

3.4. GOCE GPS-SLR residuals statistics

The SLR observations to GOCE were collected from April 2009 until October 2013 and allowed obtaining 55,336 observations, that could be used for RD orbit validation, and 52,820 observations that could be used for KIN orbit validation for the periods, when GPS orbit solutions were possible. The residual observables larger than 3

times of the standard deviation were considered as outliers. Thus, 1568 values were eliminated (1.5% of total) which gave 54,500 residuals for RD orbits and 52,088 residuals for KIN orbits. SLR observations were delivered by 19 sites, where Yarragadee provided 34% of the total amount (see Table 1). The geometric distribution of GOCE observations with different horizontal and elevation angles as seen from the stations is shown in Fig. 1. Measurements were taken at all horizontal angles, however, most of them were collected at low elevation angles between 10° and 50°. A small number of observations below 10° is related to the limitation by the station elevation mask (natural obstacles such as trees, dome's visibility limitation or hitting aircraft avoidance at low elevation angles) and were collected typically during the end parts of passes. Some of the stations track the satellites only down to 20° of the elevation angle.

Fig. 2 illustrates the SLR residual distributions for RD and KIN orbits. The statistics for the RD orbit solution show that observations from all SLR sites have the mean and the RMSE value of 0.28 ± 1.75 cm. In case of the KIN orbit solution, the observations from all SLR sites have the mean and the RMSE value of 0.13 ± 2.27 cm and they are close to the normal distribution. Those values correspond quite well to the orbit validation results obtained by Bock et al. (2014) with the mean and the RMSE value at level 0.18 ± 1.84 cm and 0.10 ± 2.42 cm for RD and KIN orbits, respectively. Differences in statistics are caused by a different threshold for outlier detection employed. We adopted tripled standard deviation value whereas Bock et al. adopted a threshold of 20 cm.

The station residual analysis for individual years between 2009 and 2013 (Fig. 3a and b) shows that in 2009 the best quality of data was delivered by the Graz station with a RMSE of 1.22 cm for RD orbit (Fig. 3a) and by Herstmonceux with a RMSE of 1.46 cm for KIN orbits (Fig. 3b), whereas the largest SLR residuals were provided by Changchun with a RMSE 2.71 cm for RD (Fig. 3a) and Hartebeesthoek with a RMSE of 2.72 cm for KIN orbits (Fig. 3b). Analyzing the mean and the RMSE values throughout the whole mission, we can see a degradation of the accuracy over time for most of the sites and for both orbit types (Fig. 3c). For the Changchun and Beijing stations, only results of the RD orbit validation is provided because in the validation of KIN orbits many outliers had to be excluded, resulting in unrealistic statistics. Note that not all stations performed measurements for the whole GOCE mission period, or collected a sufficient number of observations (e.g., Haleakala and Concepcion) to generate reliable statistics. SLR stations have different characteristics, e.g. laser pulse firing frequency rates that affect the results. The SLR normal points for GOCE are based on full rate observations averaged in the 5 s intervals. The kHz stations, such as Graz and Herstmonceux are able to collect more full rate data which contribute to the normal points than the 10 Hz stations, such as, e.g., NASA stations. Moreover, there is an obvious uneven observation distribution that might have influenced the results (see

Table 1
SLR site characteristics of the GOCE tracking.

Monument	Code	Location name, Country	Obs. No.	Percentage
7090	YARL	Yarragadee, Australia	36,355	34%
7810	ZIML	Zimmerwald, Switzerland	16,557	16%
7839	GRZL	Graz, Austria	14,911	14%
7105	GODL	Greenbelt, USA	12,423	12%
7841	POT3	Potsdam, Germany	5334	5%
7110	MONL	Monument Peak, USA	6494	6%
7840	HERL	Herstmonceux, UK	4886	5%
7237	CHAL	Changchun, China	2229	2%
7824	SFEL	San Fernando, Spain	2369	2%
7825	STL3	Mount Stromlo, Australia	2219	2%
7501	HARL	Hartebeesthoek, RSA	921	1%
7941	MATM	Matera, Italy	727	1%
8834	WETL	Wettzell, Germany	425	0.4%
7124	THTL	Tahiti, French Polynesia	298	0.3%
7308	KOGC	Koganei, Japan	158	0.1%
7249	BEIL	Beijing, China	104	0.1%
7119	HA4T	Haleakala. Maui, USA	128	0.1%
7845	GRSM	Grasse, France	42	0.0%
7405	CONL	Concepcion, Chile	8	0.0%

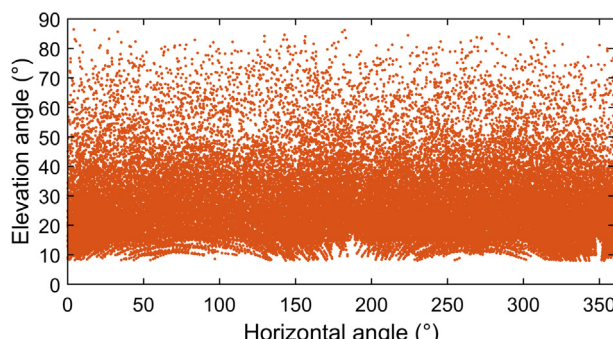


Fig. 1. Geometric distribution of GOCE observations as seen from the analyzed SLR sites.

Table 1). We decided that stations which collected fewer than 300 observations should not be considered in the analysis.

4. Results

This section compares the monthly and daily mean values of SLR residuals for RD and KIN orbit solutions to

the F10.7 cm Solar Radio Flux Index, the TEC values, and the KP index using the Pearson correlation coefficient. In case of SLR residual analysis with respect to the nadir, elevation and horizontal angles, we use a trend line fitting. First, we compare all observations w.r.t. the selected angle and then show results for chosen SLR sites. Next, we show results of SLR bias detection using SLR residuals to GPS-derived GOCE orbits. In the first step, we divide the GOCE orbits into dawn and dusk passes and analyze differences between pass types for overall observations, as well as for short period residuals with the analysis of residuals as a function of the satellite azimuth and zenith angle. The procedure in this step is advantageous for detection of station biases.

4.1. Analysis of the geomagnetic, ionospheric and solar activity influence

The Solar Radio Flux Index F10.7 cm describes the solar activity, which strongly influences the Earth's ionosphere. The F10.7 index is typically used as one of the

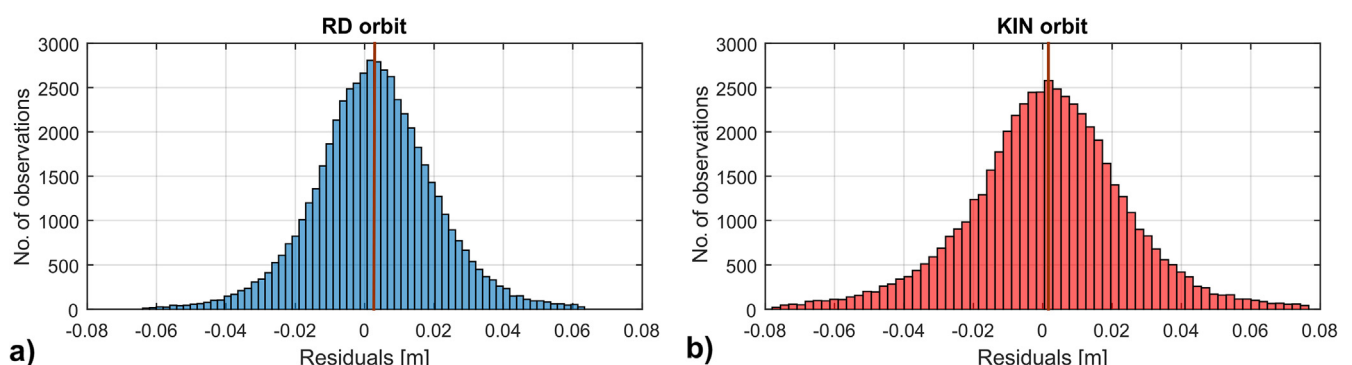


Fig. 2. Residual statistics for RD (a) and KIN (b) orbit solution (with the mean value shown as a brown line). (For interpretation of the references to colour in this figure legend, the reader is referred to the web version of this article.)



Fig. 3. Statistics of observations for individual SLR sites: a – annual RMSE for RD orbits, b – annual RMSE for KIN orbits, c – overall RMSE and biases for the entire operation phase of the mission for RD/KIN orbits.

parameters describing the air density variability of the upper atmosphere (e.g., [Vallado and Finkleman, 2014](#), [Sośnica, 2015](#)). Variations of the solar activity described

by this index have an impact on low Earth orbiting satellites because the atmospheric density and the atmospheric drag acting on satellites are directly related to the F10.7

variations. Therefore, not only LEO orbits but also geodetic parameters based on LEO's can be affected during periods of high solar activity, e.g. GRACE orbits and geocenter coordinates derived from GRACE (Tseng et al., 2017). In this study, we use the daily F10.7 values provided by the National Geophysical Data Center, USA,¹ which since 1990, have been measured at Penticton, Canada. They are adjusted to 1 AU, measured at 17:00 UT daily and expressed in units of $10^{-22} \text{ W/m}^2/\text{Hz}$.

The KP index, i.e., three-hour-range index K (Ger. *Kennziffer*) represents isolated solar particle effects on the Earth's magnetic field, by measuring the range (a difference between the highest and lowest values) during three-hourly time intervals for the most disturbed horizontal magnetic field component (Bartels et al., 1939). The KP data are provided by the German Research Centre for Geosciences² (GFZ) as collected by 13 observatories, which are located between 46° and 63° north and south geomagnetic latitude. In calculations, the daily sum of three-hour-range values is represented by the range in 28 steps from 0 (quiet) to 9 (greatly disturbed) with fractional parts expressed in thirds of a unit.

The Total Electron Content (TEC) represents a free electron amount on 1 m cross-section signal path between a satellite and a ground-based GNSS receiver. TEC is typically modeled as a vertical component and used to model the ionospheric activity. The unit of the Total Electron Content is TECU, or 10^{16} electrons/ m^2 . In this analysis, we employ 2-h global TEC values obtained from the CODE (Dach et al., 2017) for calculating daily mean values. The F10.7 and the KP were also used with data derived from GOCE in a recent study by Bruinsma et al. (2017), who employed these indices for a comparison with GOCE-derived densities at low altitudes in semi-empirical models from the COSPAR International Reference Atmosphere (CIRA).

Analysis of monthly time series and daily RMSE values to the 10.7 cm Solar Radio Flux Index shows that the quality of GPS signal, used for KIN orbit parameters determination depends on the solar activity, which is visible as an increase of the RMSE of SLR residuals and the F10.7 index values after October 2010 (see Fig. 4a). On the other hand, no significant changes of the RMSE for RD orbits are visible after October 2010, except for the last months of the mission. The correlation analysis using the Pearson correlation coefficient (PCC) gives values of 0.28 for KIN and 0.10 for RD orbits which confirms the minor sensitivity of RD orbits to the F10.7 Solar Radio Flux (Fig. 4d and g). In case of the TEC index, the results are similar (see Fig. 4b, e, h): the RMSE of SLR residuals increases after May 2011 only for KIN orbits with the PCC of 0.31, whereas there is no dependency (PCC of 0.09) for RD orbits. An increase of PCC for TEC value corresponds with

results of the correlation analysis for TEC and RD/KIN orbit differences, performed by Bock et al. (2014), where PCC values reached 0.7. Results for the KP index show a lack of correlation with PCC below 0.10 for both KIN and RD orbit (Fig. 4c, f, i).

4.2. Residuals as a function of the station nadir angle

The satellite nadir angle is the angle from the nadir direction measured in satellite center of mass to the direction of the SLR station. In the case of GOCE, the nadir angle is almost complementary to the elevation angle as seen from the SLR station, because of the very low altitude of the satellites. Comparison for all sites' trend line of residuals w.r.t. nadir angle (Fig. 5) shows a dependency between the angles of 0° and 80° at the level of $\pm 0.4 \text{ cm}$ for RD orbits and $\pm 0.8 \text{ cm}$ for KIN orbits. The comparison for single station trend line of residuals w.r.t. nadir angle (Fig. 6) shows a high dependency above a 2-cm level at several stations for both KIN and RD solutions. A large variability occurred at Monument Peak ($\sim 5 \text{ cm}$), Greenbelt ($\sim 4 \text{ cm}$), Mount Stromlo ($\sim 2 \text{ cm}$). Results for Monument Peak are very similar to those from the analysis of the differences of SLR residuals from ascending and descending passes (see Section 4.4). Such effects can be related to the satellite signature effect, i.e., to the different behavior of multi-photon SLR detectors for high return rates close to zenith and low return rates close to horizon, which is similar to that observed for flat retroreflector arrays installed on-board GNSS satellites (Sońska et al., 2015).

4.3. Residuals w.r.t. station horizontal angle

Fig. 7 illustrates the dependency between SLR residuals and horizontal angles from SLR stations to the satellite for all SLR sites. The fitted trend line (fitted sum of sine and cosine functions) of SLR residuals shows an amplitude of variations at the level of $\pm 0.5 \text{ cm}$ for RD orbits and $\pm 0.6 \text{ cm}$ for KIN orbits, which indicates that the SLR observations or GOCE orbits, especially the cross-track component, may be affected by systematic errors, e.g., due to imperfect PCV models (Bock et al., 2011). In case of single stations, the trend line of residuals comparison (Fig. 8) shows a high dependency, above the 2-cm level at several stations for both KIN and RD orbit solutions. A large variability occurs at Monument Peak ($\sim 2 \text{ cm}$), San Fernando ($\sim 2 \text{ cm}$), Graz ($\sim 1 \text{ cm}$). Large dependencies of residuals on the horizontal angle can be explained by wrong a priori station coordinates in case of Monument Peak (7110) due to post-seismic non-linear station motion (Altamimi et al., 2016). The dependency between SLR residuals and the horizontal angle can also be associated with missing horizontal gradients of the troposphere delays in SLR solutions which affect in particular observations at low elevations angles (Drożdżewski and Sońska, 2018).

¹ <http://www.ngdc.noaa.gov/ngdc.html>

² <https://www.gfz-potsdam.de/en/kp-index/>

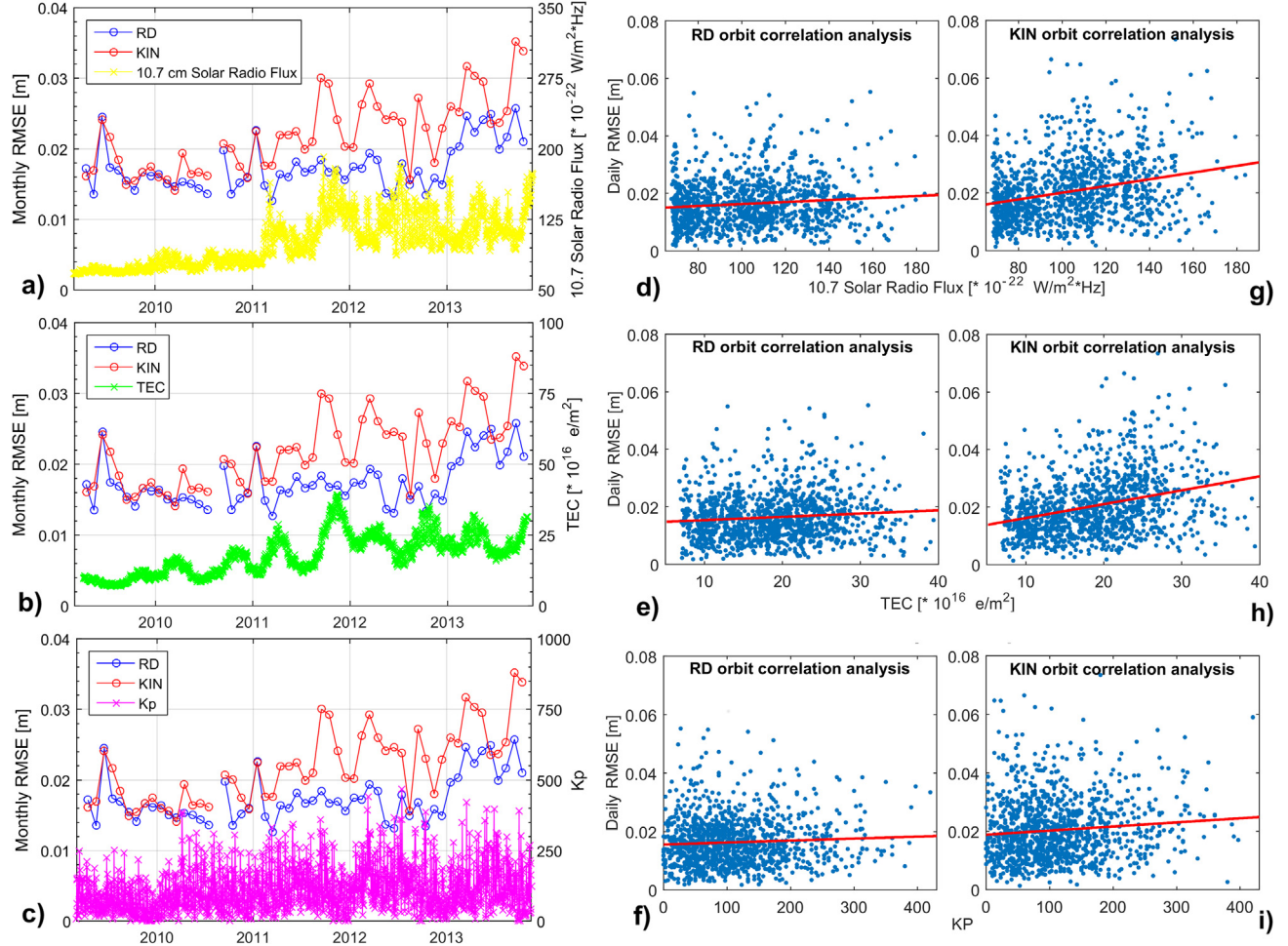


Fig. 4. Dependency between SLR RMSE and solar activity (a), ionospheric (b), and geomagnetic (c) fields with correlation analysis (d–i) for RD and KIN orbit.

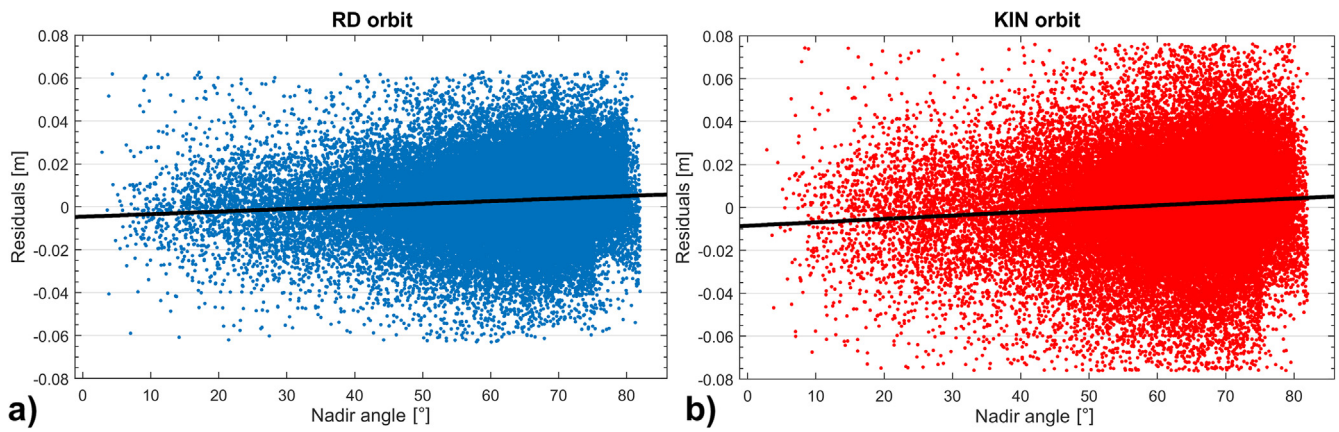


Fig. 5. SLR residuals as a function of satellite nadir angle for all SLR sites with a trend line (black).

4.4. Detection of biases using dusk and dawn passes

Sun-synchronous GOCE orbits are characterized by 2-daily passes above the same area, which allow SLR residuals to be divided into ascending (dawn) and descending (dusk) passes. We analyzed residuals divided into passes

to investigate unexpected changes, shifts or deviations, which may be caused by various effects, e.g. time biases or along-track orbit errors. Thus, for each station, observables obtained in UTC were transformed into the local solar time, considering station longitude and then partitioned into passes, considering GOCE flight direction

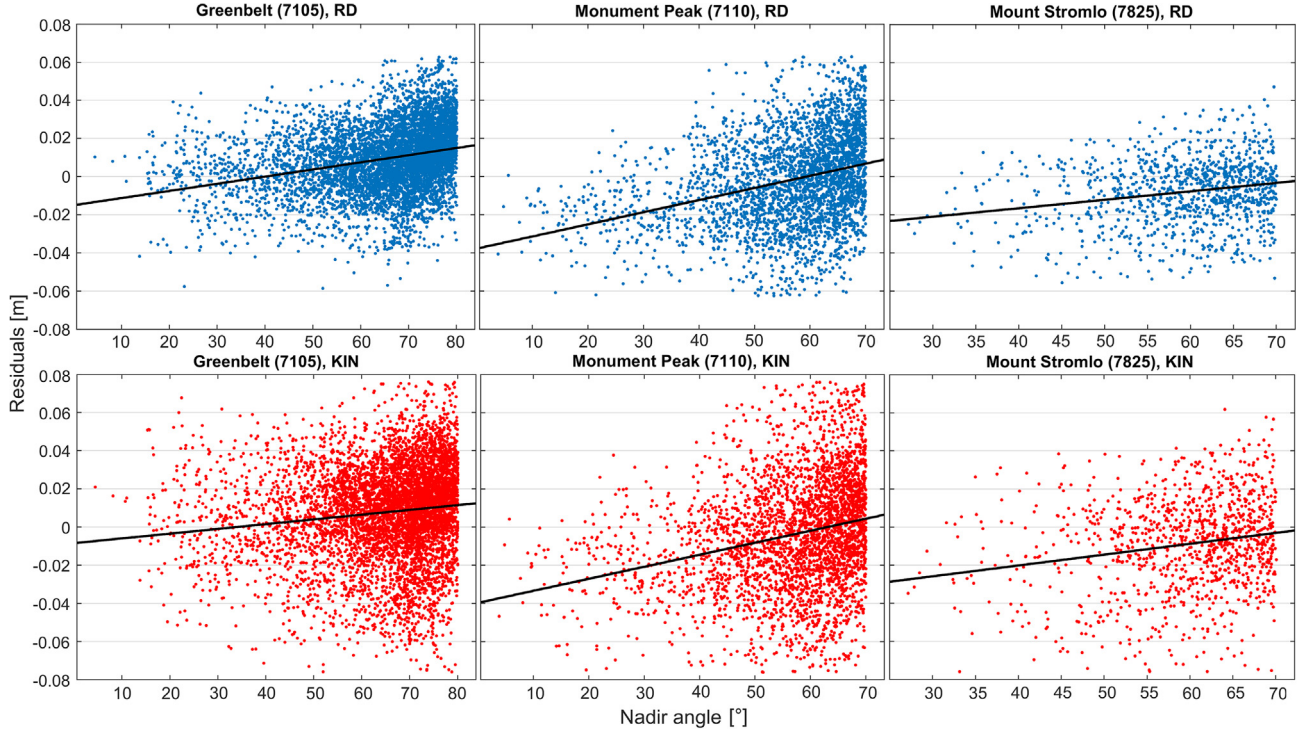


Fig. 6. SLR residuals w.r.t nadir angle for single sites: Greenbelt (7105), Monument Peak (7110), Mount Stromlo (7825) with a trend line (black).

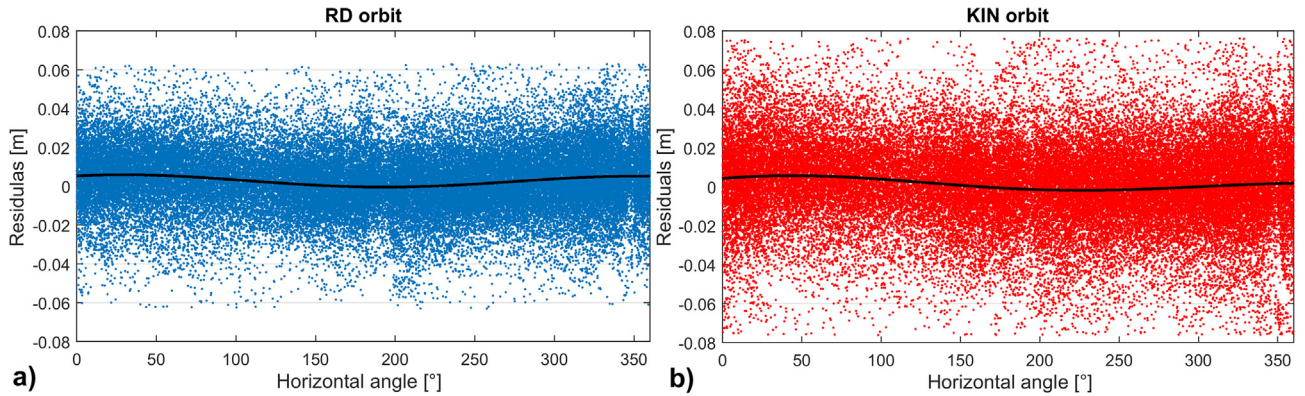


Fig. 7. Comparison of SLR residuals as a function of the horizontal angle with a trend line (fitted sine function in black).

(North-South or South-North). Nominally, the mean values of residuals for dawn and dusk pass should be at near zero level.

Results from Table 2 and Fig. 9 show that for both RD and KIN solutions, large differences between dawn and dusk passes occur, which reach cm-level. Differences of descending and ascending mean values for RD orbit (Table 2, Fig. 9) show large range bias for Monument Peak (0.94 cm), Wettzell (−0.75 cm) Hartebeesthoek (0.55 cm) and Matera (0.53 cm) sites. Very low biases occurred in Herstmonceux (−0.02 cm), Yarragadee (0.05 cm), Zimmerwald (−0.03 cm; Table 2, Fig. 9). For KIN orbit solutions, large range bias values are found in Wettzell (−1.19 cm), Monument Peak (0.98 cm), Matera (0.97 cm), Mount Stromlo (−0.69 cm), Hartebeesthoek (0.63 cm) and San

Fernando (0.52 cm, see Table 2, Fig. 9). Lowest mean residuals occurred in Greenbelt, Potsdam (−0.01 cm, see Table 2, Fig. 9).

When two kinds of passes have mean values with opposite signs and large differences, it can be assumed that an along-track bias may have occurred. SLR stations provided more observations during the end of each GOCE pass than during the initial part of the pass, which causes an inhomogeneous observation geometry, which may map into dawn/dusk pass differences. Thus, those sites which indicate a large difference between two pass types, indicate an orbit along-track error or they may be affected by UTC time synchronization error, i.e., a time bias, when the distribution of SLR observations during dawn and dusk passes is uneven, and the same error is registered

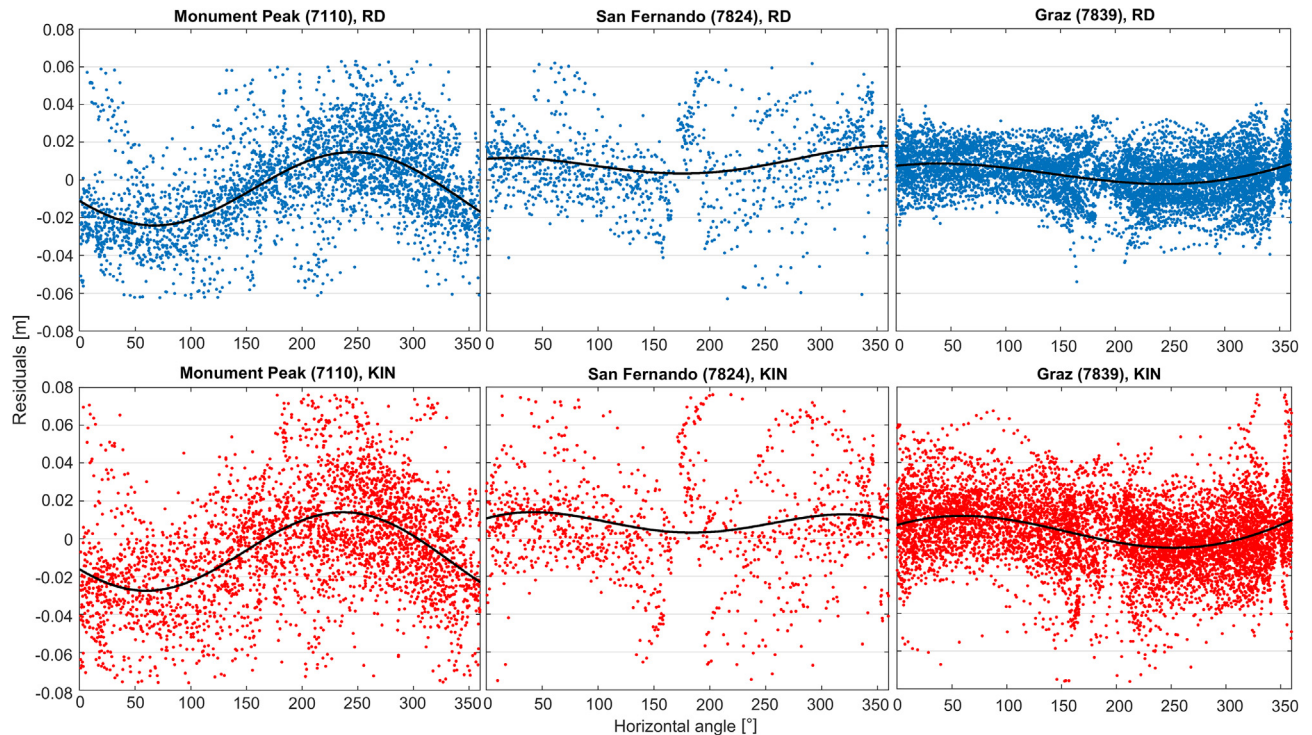


Fig. 8. Comparison of residuals as a function of the horizontal angle with trend line (fitted sine function in black) for selected stations: Monument Peak (7110), San Fernando (7824), Graz (7839).

Table 2

Results of mean residual and time bias value from overall mission data for all SLR stations (in italic results with unreliable, low number of observations).

Monument	Location name	Mean residual values [cm]				Difference between dawn and dusk passes [cm]	
		RD		KIN		RD	KIN
		Dawn pass	Dusk pass	Dawn pass	Dusk pass		
7090	Yarragadee	-0.05	-0.10	-0.20	-0.09	0.05	-0.11
7810	Zimmerwald	0.31	0.34	0.33	0.23	-0.03	0.10
7839	Graz	0.35	0.23	0.43	0.24	0.12	0.19
7105	Greenbelt	0.63	0.83	0.57	0.58	-0.20	-0.01
7841	Potsdam	0.41	0.30	0.26	0.27	0.11	-0.01
7110	Monument Peak	0.36	-0.58	0.17	-0.81	0.94	0.98
7840	Herstmonceux	0.74	0.72	0.81	0.65	0.02	0.16
7237	Changchun	1.56	1.26	—	—	0.30	—
7824	San Fernando	0.65	0.85	1.12	0.60	-0.20	0.52
7825	Mount Stromlo	-0.97	-0.54	-1.15	-0.46	-0.43	-0.69
7501	Hartebeesthoek	0.97	0.42	0.86	0.23	0.55	0.63
7941	Matera	1.00	0.47	1.08	0.11	0.53	0.97
8834	Wettzell	0.66	1.41	0.59	1.78	-0.75	-1.19
7124	Tahiti	0.82	-0.20	3.14	-2.18	1.02	5.32
7308	Koganei	-1.96	0.30	-3.73	0.14	-2.26	-3.87
7249	Beijing	-4.80	0.91	—	—	-5.71	—

for KIN and RD orbits. When this error is observed only for one kind of the orbit, e.g., KIN, it should be assigned to the particular orbit type. Moreover, most of the SLR stations provide slightly more observations during the dusk passes because dawn passes typically are during or just before observers' shifts at SLR stations. Most of the stations like Greenbelt, Graz, Yarragadee, Zimmerwald, Potsdam appear not to be affected by this error because the difference between dusk and dawn passes is close to zero.

4.5. Satellite single pass investigation

In a further analysis, the characteristics of single passes above stations were investigated. We divided results into passes which may be affected by various factors including orbit errors or with unknown residual distribution (Fig. 10) and possibly affected by a time bias to the greatest extent (Fig. 11). In Fig. 10 we show results for passes with large residual differences between KIN and RD (few-cm

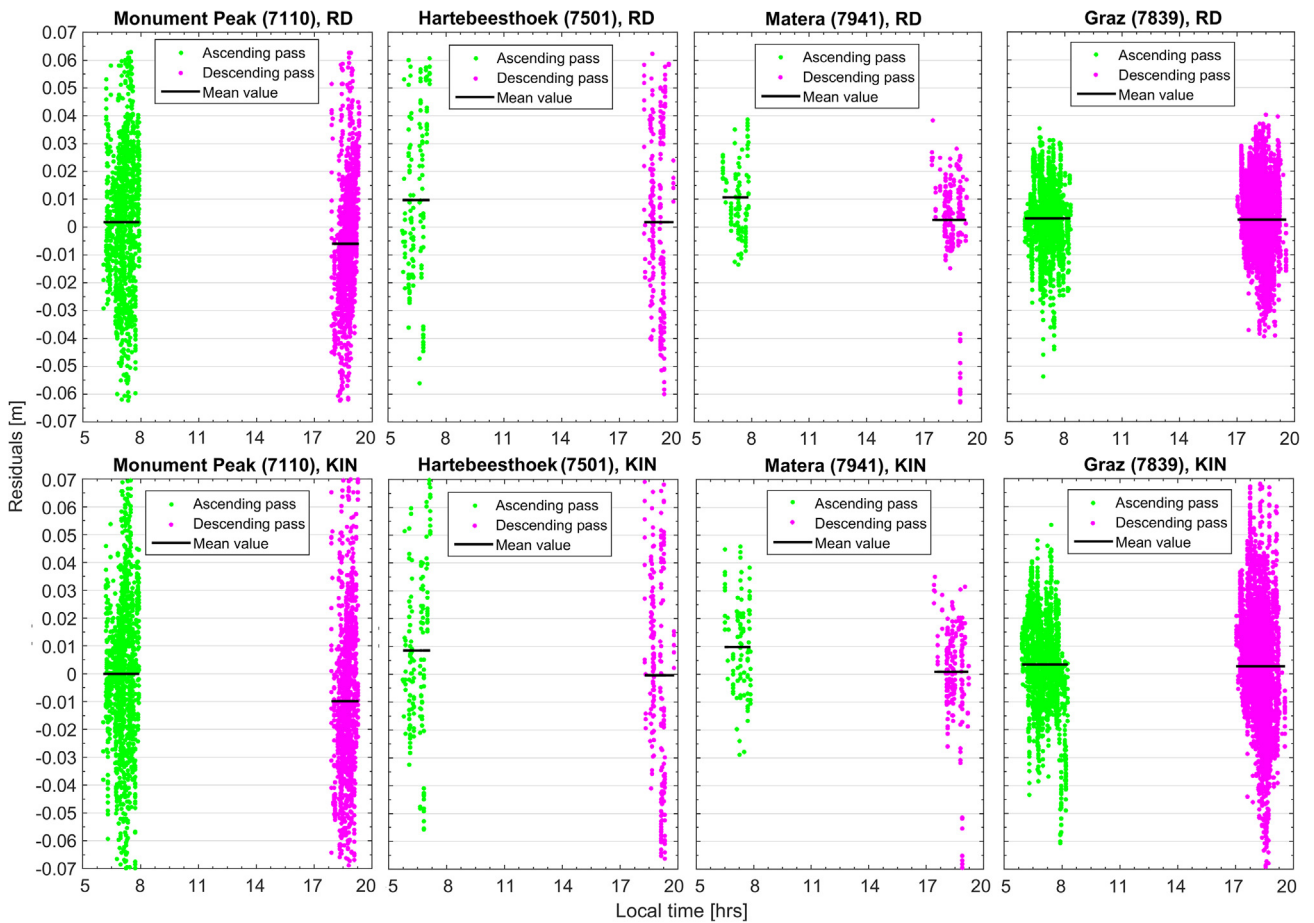


Fig. 9. Residuals for dawn (green) and dusk (magenta) passes with mean values (black) from overall mission data for Monument Peak (7110), Hartebeesthoek (7501), Matera (7941) and Graz (7839). (For interpretation of the references to colour in this figure legend, the reader is referred to the web version of this article.)

level). These large errors are due to wrong orbit determination, in most cases wrong KIN orbits, because KIN orbits are affected by larger slopes and offsets than RD orbits. Smaller errors contributing to large SLR residuals may be caused by: a time bias, a range bias, wrong a priori station coordinates, deficiencies in troposphere delay modeling etc. For KIN orbit solutions, we noticed higher differences of residuals (i.e. Potsdam on October 2, 2012; Yarragadee on October 28, 2011; Zimmerwald on October 15, 2010; see Fig. 10) and higher variations of residuals (i.e. Zimmerwald on March 24, 2012; Graz on September 21, 2011; Monument Peak on September 23, 2010; Wettzell on March 22, 2012; Fig. 10) than in case of RD solution. Looking at the SLR residuals from Zimmerwald (7810) collected on March 24, 2012, or Graz (7839) collected on September 21, 2011, it is clear that the KIN orbit is strongly affected by the along-track systematic error, which might be caused by ionosphere activity changes affecting GPS signal and consequently also KIN positions. No sensitivity to such effect can be seen for RD orbit, because the same SLR residuals are used to validate both orbit types at the same epochs. Residuals patterns with large slopes over time, such as in case of Monument Peak (7110), indicate

along-track errors in case of KIN orbits. Patterns with a systematic shift between RD and KIN orbits, such as for Yarragadee (7090) and Potsdam (7841) indicate radial orbit errors, which may exceed the value of 6 cm (even when RD and KIN orbits are based on exactly the same set of GPS observations). Thus, SLR can be used for identifying orbit errors even in short time spans on the basis of single passes.

In Fig. 11 we present passes whose residual differences and distribution may be mostly caused by time biases at the SLR stations. We compared ascending (dawn) and descending (dusk) passes from corresponding periods, assuming similar tracking conditions. Sometimes it was impossible to find stations which collected observation for dawn and dusk passes at the same day, thus, data from neighboring days were used. For the analyzed short-time (less than a few days) dawn and dusk passes, we noticed a significant change of the residual sign (or amplitude) during a single pass. For Graz, Yarragadee, Greenbelt, Monument Peak and Zimmerwald sites we found daily passes with 2–5 cm residual differences with a characteristic sign change occurring when the satellite was close to the zenith. For example, in case of the dawn pass, when the satellite

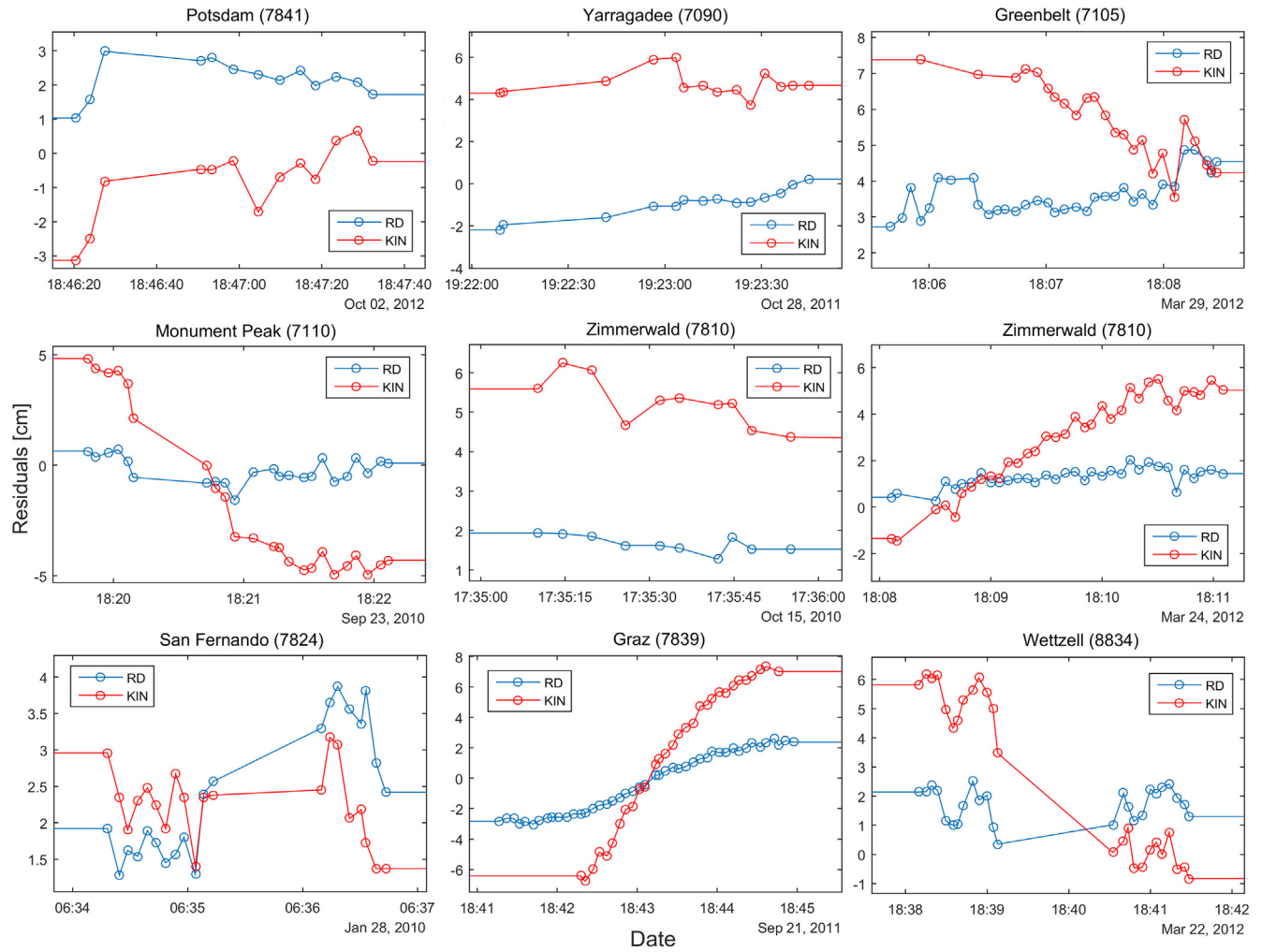


Fig. 10. Single satellite passes with large residual differences for RD and KIN orbit.

was approaching the SLR site, the residuals had a different sign comparing to moment when satellite was receding from the SLR site (Fig. 11a–e left). An analogue behavior occurred during dusk pass (see Fig. 11a–e right). The residual value distribution expressed as a function of the station azimuth and zenith angle (Fig. 11f–j) shows that the residual sign change occurs when the satellite is approaching the zenith direction. It should be noted that the time bias error may also have different characteristics than described here and the observed patterns may also be associated with common along-track errors or cross-track errors for RD and KIN orbits. However, the pattern observed in Fig. 11 is also typical for time biases at SLR stations and can be converted into the time bias values occurring at the stations (Otsubo et al., 2018). Therefore, the analysis of precise GOCE orbits can be used for the identification of various systematic effects affecting the stations, including the time biases.

5. Summary

In this paper, the SLR residuals of GPS-based GOCE orbits are used to analyze their dependency on ionospheric,

solar, and geomagnetic activities and systematic errors of SLR stations. For the entire mission duration, the mean SLR residuals are oscillating near zero, while the RMSE is at near 2-cm level for KIN and RD orbits. In case of single site analysis, we found that some of the stations might be affected by systematic errors, such as time and range biases, which are detected for Hartebeesthoek, Monument Peak, San Fernando. The analysis of mean SLR observation residuals as a function of solar and ionospheric field activity indices, i.e., F10.7 Solar Radio Flux and TEC, shows that GPS signal, which is used for determination of the KIN positions are susceptible to variations of the solar and ionospheric activities, while the RD orbits are largely resistant. The TEC correlation results show consistency with those made by Bock et al. (2014), despite the fact that SLR-GNSS residuals are affected by more systematic errors. No significant dependency was found between the magnetic field activity measured by KP index neither for KIN nor for RD orbit solutions.

The low GOCE altitude implies that the satellite passes the thermosphere with variable densities which causes irregular drag. The atmospheric drag should be measured by GOCE accelerometers and compensated by dedicated

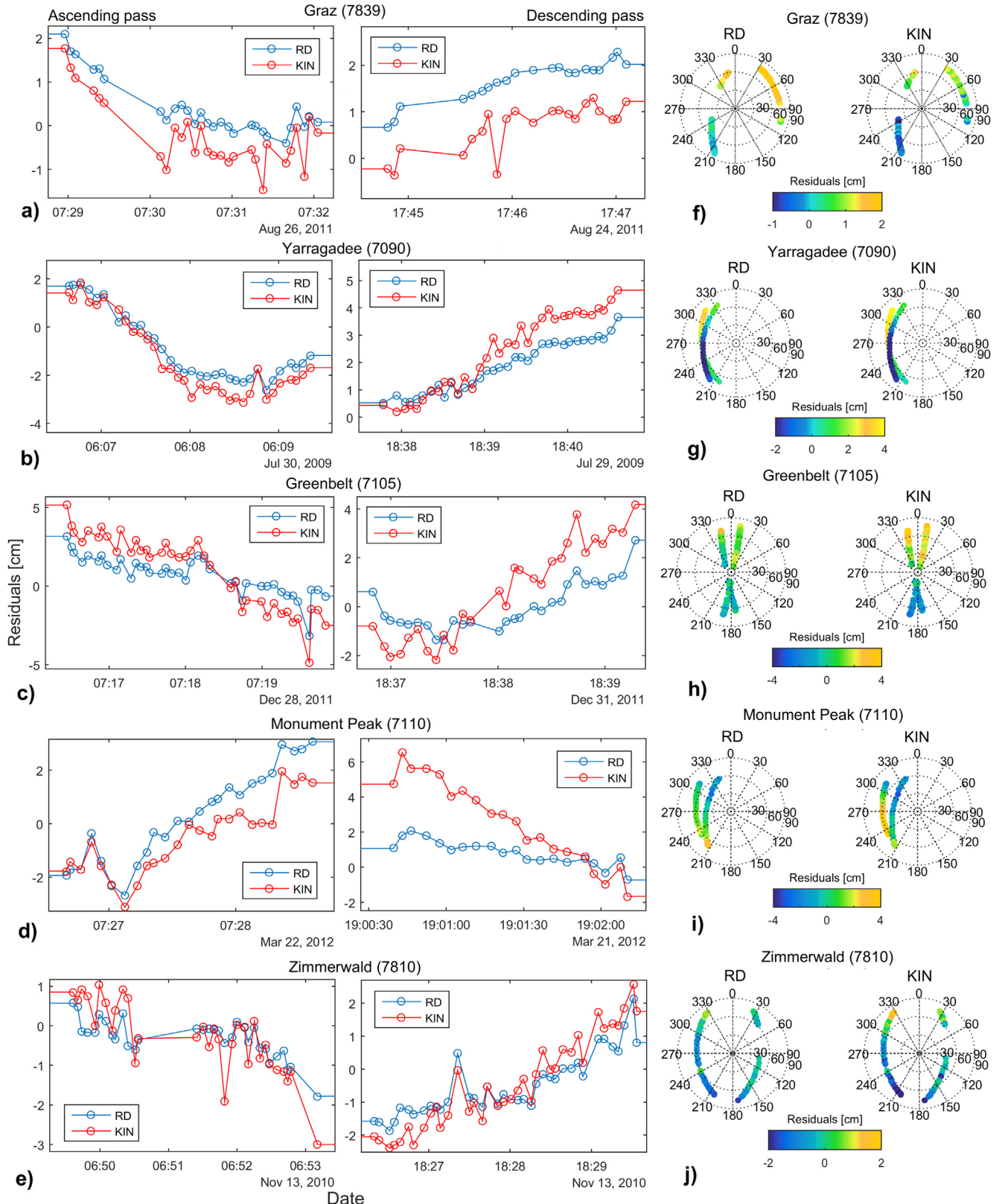


Fig. 11. Examples of satellite passes where SLR site may be affected by time bias error (a–e, left – dawn pass; a–e, right – dusk pass; f–j – distribution through GOCE satellite azimuth and zenith angle).

thrusters. In case of KIN orbit solution, due to its geometrical approach, atmospheric drag should not affect satellite position. For RD approach, this effect may influence the

solution when non-conservative forces are not observed by an accelerometer or not compensated by dedicated pseudo-stochastic accelerations. However, if accelerometer

measurements are included in the estimation of the RD orbit, air drag has almost no effect on the results for the RD orbit. Therefore, we can conclude that the dominating error in the GPS-derived orbital parameters is most likely an error in the GPS signal and consequently in the GPS observations, because the KIN orbit is more affected by ionospheric variations than the RD orbit. The consequences of atmospheric density variations are not observed in RD orbits, because they were compensated by the mission drag-free control mode, whereas the remaining non-conservative forces were absorbed by estimated empirical accelerations.

The altitude of the GOCE satellite was lowered several times during the mission. Despite variable satellite heights and various ionospheric activity between 2009 and 2013, no notable degradation of RD orbit quality was detected. The quality of RD orbits, which were parametrized fully empirical, regarding the non-gravitational forces, was persistent and constant during the whole GOCE mission, partly due to the drag-free control flight mode. The drag-free mode compensated already large parts of forces affecting atmospheric density, which is indirectly dependent upon higher ionospheric and geomagnetic activity. Therefore, we may conclude that the GOCE RD orbits used in this study are insensitive to satellite altitude, solar activity, ionospheric activity, and geomagnetic activity.

A method of the detection of SLR time biases using the analysis of SLR residuals from ascending and descending passes of GOCE sun-synchronous orbits showed that some stations, e.g., Hartebeesthoek and Matera, might be affected by time bias errors. Results from the analysis of SLR station residuals as a function of the nadir angle and horizontal angle of the SLR observations show a high variability at 2–4 cm level for Monument Peak, Greenbelt and Mount Stromlo. Differences of SLR residuals between KIN and RD orbits show that KIN orbits are much more often affected by radial errors (registered as a constant shift of residuals) and along-track errors (registered as varying south-north residuals with a residual sign change in zenith) or cross-track errors (visible especially as differences between east-west directions). Residual patterns at some stations, e.g., Monument Peak, indicate that these stations can also be affected by wrong station coordinates and deficiencies in troposphere delay modeling, e.g., missing horizontal gradients of the troposphere delay.

Acknowledgments

The authors gratefully acknowledge the Astronomical Institute, University of Bern (AIUB) for providing GOCE orbits and to all members of the International Satellite Laser Ranging Service for their effort to collect and provide SLR observations of LEO satellites. Their work provides the basis for the present study and is an essential contribution to numerous space missions. We also appreciate three anonymous reviewers and the responsible editor for their valuable comments and improvements to this manuscript.

References

- Altamimi, Z., Collilieux, X., Métivier, L., 2011. ITRF2008: an improved solution of the international terrestrial reference frame. *J. Geod.* 85 (8), 457–473. <https://doi.org/10.1007/s00190-011-0444-4>.
- Altamimi, Z., Rebischung, P., Métivier, L., Collilieux, X., 2016. ITRF2014: a new release of the International Terrestrial Reference Frame modeling nonlinear station motions. *J. Geophys. Res. Solid Earth* 121, 6109–6131. <https://doi.org/10.1002/2016JB013098>.
- Arnold, D., Montenbruck, O., Hackel, S., Sośnica, K., 2018. Satellite laser ranging to low Earth orbiters: orbit and network validation. *J. Geod.* 2018, 1–18. <https://doi.org/10.1007/s00190-018-1140-4>.
- Bartels, J., Heck, N.H., Johnston, H.F., 1939. The three-hour-range index measuring geomagnetic activity. *Terr. Magn. Atmos. Electr.* 44, 411–454. <https://doi.org/10.1029/TE044i004p00411>.
- Bock, H., Dach, R., Jäggi, A., Beutler, G., 2009. High-rate GPS clock corrections from CODE: support of 1 Hz applications. *J. Geod.* 83, 1083. <https://doi.org/10.1007/s00190-009-0326-1>.
- Bock, H., Jäggi, A., Meyer, U., Dach, R., Beutler, G., 2011. Impact of GPS antenna phase center variations on precise orbits of the GOCE satellite. *Adv. Space Res.* 47, 1885–1893. <https://doi.org/10.1016/j.asr.2011.01.017>.
- Bock, H., Jäggi, A., Beutler, G., Meyer, U., 2014. GOCE: precise orbit determination for the entire mission. *J. Geod.* 88, 1047–1060. <https://doi.org/10.1007/s00190-014-0742-8>.
- Bruinsma, S., Arnold, D., Jäggi, A., Sánchez-Ortiz, N., 2017. Semi-empirical thermosphere model evaluation at low altitude with GOCE densities. *J. Space Weather Space Clim.* 7, A4. <https://doi.org/10.1051/swsc/2017003>.
- Dach, R., Brockmann, E., Schaer, S., Beutler, G., Meindl, M., Prange, L., Bock, H., Jäggi, A., Ostini, L., 2009. GNSS processing at CODE: status report. *J. Geod.* 83 (3–4), 353–365. <https://doi.org/10.1007/s00190-008-0281-2>.
- Dach, R., Lutz, S., Walser, P., Frizez, P. (Eds), 2015. Bernese GNSS Software Version 5.2. User manual, Astronomical Institute, University of Bern, Bern Open Publishing. doi:10.7892/boris.72297. (ISBN: 978-3-906813-05-9).
- Dach, R., Schaer, S., Arnold, D., Prange, L., Sidorov, D., Sušnik, A., Villiger, A., Jäggi, A., 2017. CODE final product series for the IGS. Published by Astronomical Institute, University of Bern. doi:10.7892/boris.75876.2 URL: <<http://www.aiub.unibe.ch/download/CODE>>.
- Drinkwater, M., Haagmans, R., Muzi, D., Popescu, A., Floberghagen, R., Kern, M., Fehringer, M., 2006. The GOCE gravity mission: ESA's first core explorer. In: Proceedings of the 3rd GOCE User Workshop, 6–8 Nov 2006, Frascati, Italy, ESA SP-627, pp. 1–7.
- Drożdżewski, M., Sośnica, K., 2018. Satellite laser ranging as a tool for the recovery of tropospheric gradients. *Atmos. Res.* 212, 33–42. <https://doi.org/10.1016/j.atmosres.2018.04.028>.
- European Space Agency, 1998. The Science and Research Elements of ESA's Living Planet Programme, ESA SP-1227, 105.
- Exertier, P., Belli, A., Lemoine, J.M., 2017. Time biases in laser ranging observations: a concerning issue of space geodesy. *Adv. Space Res.* 60 (5), 948–968. <https://doi.org/10.1016/j.asr.2017.05.016>.
- Exertier, P., Belli, A., Samain, E., Meng, W., Zhang, H., Tang, K., Sun, X., 2018. Time and laser ranging: a window of opportunity for geodesy, navigation, and metrology. *J. Geod.* <https://doi.org/10.1007/s00190-018-1173-8>.
- Floberghagen, R., Fehringer, M., Lamarre, D., Muzi, D., Frommknecht, B., Steiger, C., Piñeiro, J., Da Costa, A., 2011. Mission design, operation and exploitation of the gravity field and steady-state ocean circulation explorer mission. *J. Geod.* 85 (11), 749–758. <https://doi.org/10.1007/s00190-011-0498-3>.
- GOCE Flight Control Team, 2014. GOCE End-of-Mission Operations Report. European Space Agency ESA.
- Hadas, T., Krzyplak-Gregorczyk, A., Hernández-Pajares, M., Kaplon, J., Paziewski, J., Wielgosz, P., Orus-Perez, R., 2017. Impact and implementation of higher-order ionospheric effects on precise GNSS

- applications. *J. Geophys. Res.: Solid Earth* 122, 9420–9436. <https://doi.org/10.1002/2017JB014750>.
- ILRS Analysis Standing Committee, 2016. SLRF2008. <<https://ilreddis.eosdis.nasa.gov/science/awg/SLRF2008.html>>. (Accessed 9 Apr 2018).
- Jäggi, A., Hugentobler, U., Beutler, G., 2006. Pseudo-stochastic orbit modeling techniques for low-Earth orbiters. *J. Geod.* 80 (1), 47–60. <https://doi.org/10.1007/s00190-006-0029-9>.
- Jäggi, A., 2007. Pseudo-Stochastic Orbit Modeling of Low Earth Satellites Using the Global Positioning System. *Geodätisch-geophysikalische Arbeiten in der Schweiz*, vol. 73, Schweizerische Geodätische Kommission.
- Jäggi, A., Bock, H., Pail, R., Goiginger, H., 2008. Highly reduced-dynamic orbits and their use for global gravity field recovery: a simulation study for GOCE. *Stud. Geophys. et Geodaetica* 52 (3), 341–359. <https://doi.org/10.1007/s11200-008-0025-z>.
- Jäggi, A., Bock, H., Floberghagen, R., 2011. GOCE orbit predictions for SLR tracking. *GPS Solut.* 15, 129. <https://doi.org/10.1007/s10291-010-0176-6>.
- Luceri, V., Bianco, G., 2008. The temporary ILRS reference frame: SLRF2005, presented at ILRS Fall Meeting, 24–28 September 2007, Grasse. <http://ilrs.gsfc.nasa.gov/docs/2007/AWG_GRASSE_24.09.2007.pdf>
- Mendes, V., Pavlis, E., 2004. High-accuracy zenith delay prediction at optical wavelengths. *Geophys. Res. Lett.* 31 (14). <https://doi.org/10.1029/2004GL020308>.
- Montenbruck, O., Neubert, R., 2011. Range correction for the CryoSat and GOCE laser retro-reflector arrays. Technical Note DLR/GSOC11-01.
- Otsubo, T., Mueller, H., Pavlis, E.C., Torrence, M., Thaller, D., Glotov, V., Wang, X., Sośnica, K., Meyer, U., Wilkinson, M., 2018. Rapid Response Quality Control Service for the Laser Ranging Tracking Network. *J. Geod.* (in press).
- Pearlman, M., Degnan, J., Bosworth, J., 2002. The International Laser Ranging Service. *Adv. Space Res.* 30 (2), 135–143. [https://doi.org/10.1016/S0273-1177\(02\)00277-6](https://doi.org/10.1016/S0273-1177(02)00277-6).
- Rebischung, P., Griffiths, J., Ray, J., Schmid, R., Collilieux, X., Garayt, B., 2012. IGS08: the IGS realization of ITRF2008. *GPS Solutions* 16, 483–494. <https://doi.org/10.1007/s10291-011-0248-2>.
- Rummel, R., Balmino, G., Johannessen, J., Visser, P., Woodworth, P., 2002. Dedicated gravity field missions—principles and aims. *J. Geodyn.* 33, 3–20. [https://doi.org/10.1016/S0264-3707\(01\)00050-3](https://doi.org/10.1016/S0264-3707(01)00050-3).
- Samain, E., Exertier, P., Courde, C., Fridelance, P., Guillemot, P., Laas-Bourez, M., Torre, J.M., 2015. Time transfer by laser link: a complete analysis of the error budget. *Metrologia* 52, 423–432. <https://doi.org/10.1088/0026-1394/52/2/423>.
- Sośnica, K., 2015. Impact of the atmospheric drag on Starlette, Stella, Ajisai and Lares Orbits. *Artificial Satellites* 50 (1), 1–18. <https://doi.org/10.1515/arsa-2015-0001>.
- Sośnica, K., Thaller, D., Dach, R., Steigenberger, P., Beutler, G., Arnold, D., Jäggi, A., 2015. Satellite laser ranging to GPS and GLONASS. *J. Geod.* 89 (7), 725–743. <https://doi.org/10.1007/s00190-015-0810-8>.
- Švehla, D., Rothacher, M., 2005. Kinematic precise orbit determination for gravity field determination. In: Sansò, F. (Ed.), *A Window on the Future of Geodesy*. Springer, Berlin Heidelberg, pp. 181–188. https://doi.org/10.1007/3-540-27432-4_32.
- Tseng, T.-P., Hwang, C., Sosnicka, K., Kuo, C.-Y., Liu, Y.-C., Yeh, W.-H., 2017. Geocenter motion estimated from GRACE orbits: the impact of F10.7 solar flux. *Adv. Space Res.* 59 (11), 2819–2830. <https://doi.org/10.1016/j.asr.2016.02.003>.
- Vallado, D.A., Finkleman, D., 2014. A critical assessment of satellite drag and atmospheric density modeling. *Acta Astronautica* 95, 141–165. <https://doi.org/10.1016/j.actaastro.2013.10.005>.
- Visser, P.N.A.M.J., van den IJssel, T., Van Helleputte, H., Bock, A., Jäggi, G., BeutlerŠvehla, D., Hugentobler, U., Heinze, M., 2009. Orbit determination for the GOCE satellite. *Adv. Space Res.* 43, 760–768. <https://doi.org/10.1016/j.asr.2008.09.016>.
- Willis, P., Delefie, F., Barlier, F., Bar-Sever, Y.E., Romans, L.J., 2005. Effects of thermosphere total density perturbations on LEO orbits during severe geomagnetic conditions (Oct–Nov 2003) using DORIS and SLR data. *Adv. Space Res.* 36 (3), 522–533. <https://doi.org/10.1016/j.asr.2005.03.029>.
- Willis, P., Heflin, M.B., Haines, B.J., Bar-Sever, Y.E., Bertiger, W.I., Mandea, M., 2016. Is the Jason-2 DORIS oscillator also affected by the South Atlantic Anomaly? *Adv. Space Res.* 58 (12), 2617–2627. <https://doi.org/10.1016/j.asr.2016.09.015>.
- Wu, S., Yunck, T., Thornton, C., 1991. Reduced-dynamic technique for precise orbit determination of low Earth satellites. *J. Guid. Control Dyn.* 14 (1), 24–30.
- Zin, A., Landenna, S., Conti, A., 2006. Satellite to satellite tracking instrument. In: Proc. 3rd Int. GOCE User Workshop.